AIP Journal of Applied Physics

Intensity-dependent equivalent circuit parameters of organic solar cells based on pentacene and C60

Seunghyup Yoo, Benoit Domercq, and Bernard Kippelen

Citation: J. Appl. Phys. 97, 103706 (2005); doi: 10.1063/1.1895473
View online: http://dx.doi.org/10.1063/1.1895473
View Table of Contents: http://jap.aip.org/resource/1/JAPIAU/v97/i10
Published by the American Institute of Physics.

JOURNAL OF APPLIED PHYSICS **97**, 103706 (2005)

Intensity-dependent equivalent circuit parameters of organic solar cells based on pentacene and C_{60}

Seunghyup Yoo, Benoit Domercq, and Bernard Kippelen[a)]
Center for Organic Photonics and Electronics (COPE), School of Electrical and Computer Engineering, Georgia Institute of Technology, Atlanta, Georgia 30332

(Received 2 December 2004; accepted 26 February 2005; published online 2 May 2005)

We present studies of the current–voltage characteristics of organic solar cells based on heterojunctions of pentacene and C_{60} as a function of illumination intensity. The photovoltaic response at a given illumination level is parameterized and modeled using the equivalent circuit model developed for inorganic *pn*-junction solar cells. Reduction in shunt resistance and increase in diode reverse saturation current density are observed upon increase of the light intensity. We demonstrate that this effect can be modeled by a refined equivalent circuit model that contains an additional shunt resistance and an additional diode the properties of which are functions of the light intensity. The effects of these additional components on the overall photovoltaic performance are discussed. © *2005 American Institute of Physics*. [DOI: 10.1063/1.1895473]

I. INTRODUCTION

In recent years, interest in solid-state organic solar cells has grown considerably due to their possibilities to be fabricated onto light-weight conformable substrates, using low-temperature processing techniques potentially at low cost. Currently, this class of solar cells has reached power conversion efficiencies of a few percents. Organic excitonic solar cells are typically comprised of small molecular weight multilayer thin films,[1–3] interpenetrating polymer blend bulk heterojunctions,[4–6] organic/nanocrystal bulk heterojunctions,[7] or organic/TiO_2 heterojunctions.[8,9] Photovoltaic energy conversion in both multilayer devices and blend devices rely mainly on heterojunctions formed between donor and acceptor materials. Recently, we have demonstrated that multilayer thin-film solar cells based on heterojunctions of pentacene as donor and C_{60} as acceptor can be a promising platform for efficient light harvesting partly because of the relatively large exciton diffusion length of excitons in pentacene and because of the efficient dissociation of excitons at the heterojunction formed with C_{60}.[10]

In this paper, we present studies on the dependence of the electrical characteristics of organic solar cells based on such pentacene/C_{60} heterojunctions as a function of light intensity. First, current–voltage (J–V) characteristics are modeled in a wide range of voltage. For each illumination intensity, the well-known equivalent-circuit model used for inorganic solar cells[11] is applied to parameterize the electrical characteristics in terms of the equivalent-circuit parameters, including the diode parameters such as the ideality factor n and the reverse saturation current density J_S, the photocurrent J_{ph} delivered by the current source, and the different equivalent resistances such as series resistance R_S and shunt resistance R_P. These parameters are important as they are related to experimental parameters, including the open-circuit voltage (V_{OC}), the short-circuit current density (J_{SC}), and the fill factor (FF) of the device. When the illumination is varied, we find a reduction in shunt resistance and an increase in the diode reverse saturation current density upon increase of the light intensity. We propose modifications to the equivalent-circuit model and show that an additional shunt resistance and intensity-dependent diode parameters can describe these light-dependent processes. Finally, we quantitatively analyze the effects of these light-dependent processes on the overall photovoltaic performance.

II. EXPERIMENTS

The devices under study consist of multilayer organic films deposited on a glass substrate precoated with indium tin oxide (ITO) with an aluminum (Al) top electrode, as shown in Fig. 1(a). ITO (15 Ω per square) was used as-

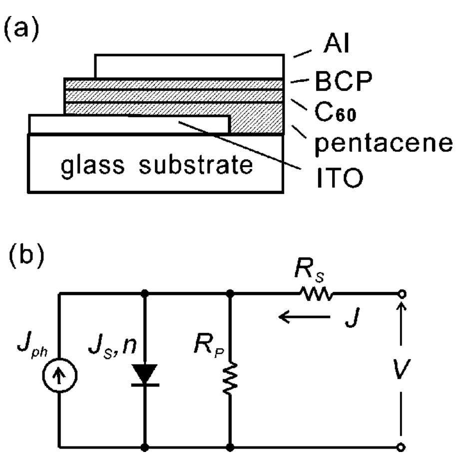

FIG. 1. (a) Schematic structure of a device. Organic and metal layers are deposited in sequence on top of a precleaned ITO glass by physical vapor deposition in vacuum. Thin layer of bathocuproine (BCP) is used as an exciton-blocking layer, as suggested in Ref. 2. The overlap area between aluminum (Al) and ITO electrodes define a device area which is typically ~0.1 cm^2. (b) Equivalent circuit typically used for *pn*-junction solar cells. J_{ph} is photo-generated current density, J_S and n are the reverse saturation current density and the ideality factor of a diode, respectively, and R_S and R_P are series and shunt resistances.

[a)]Author to whom correspondence should be addressed; electronic mail: Kippelen@ece.gatech.edu received, without further treatment except for routine cleaning procedure. Part of the ITO was etched, and the overlap area between the ITO and Al electrodes defined devices with an area A of typically $\sim 0.1\ \mathrm{cm}^2$.

A thin layer of bathocuproine (BCP) was inserted between C_{60} and Al as an exciton-blocking layer to prevent excitons created in the C_{60} layer from being quenched in the vicinity of the metal, and to protect the C_{60} layer from being damaged upon deposition of Al.[2] All the organic materials were purified once by thermal gradient sublimation[12] in vacuum before use. The organic layers and the Al electrode were deposited in sequence through shadow masks onto ITO substrates by the physical vapor deposition. The typical vacuum was 10^{-7} Torr or less during the deposition of the organic materials.

The devices were never exposed to air, and their photovoltaic properties were measured in nitrogen. The filtered output of a 175-W Xenon lamp (CVI, model ASB-XE-175EX) was used as a broadband light source (350–900 nm). The intensity of the incident light (I_L) was measured with a calibrated Si photodiode (detector area $=0.13\ \mathrm{cm}^2$) with known spectral response. The spectrum of the light source was measured using a charge-coupled device (CCD)-based spectrometer (Ocean Optics, USB 2000). The current–voltage characteristics were measured with a Keithley 2400 source meter in a four-wire connection scheme to avoid the effect of the voltage drop due to the resistances associated with the probe lines and the electrical connection.

III. THEORY

A. Equivalent circuit model for solar cells: Basic formulation

Approaches utilizing an equivalent circuit are known to be useful in analyzing and parameterizing the electrical characteristics of inorganic *pn*-junction solar cells,[11,13] and have also been applied to organic solar cells.[3,14–19] As shown in Fig. 1(b), the circuit is comprised of a diode, a dc current source, a shunt resistance R_P, and a series resistance R_S. The current density of the dc current source corresponds to the photocurrent density J_{ph}. The diode is characterized by its reverse saturation current density J_S and ideality factor n. R_P takes into account the loss of carriers via the leakage paths that may be created, for example, through pinholes in the film. On the other hand, R_S is attributed to the bulk resistivity of the semiconducting materials, the contact resistance between the semiconductors and the adjacent electrodes, and the resistance associated with probe lines and interconnections.[11,13,20] Provided that the dark characteristic is reasonably modeled using this equivalent circuit with $J_{ph}=0$, then the electrical characteristic under illumination I_L can be easily obtained once the functional relation of J_{ph} to I_L is known. In typical inorganic *pn*-junction solar cells, $J_{ph}(I_L)$ is regarded linear.

In the equivalent circuit model, the current–voltage characteristic is described by[11]

$$J = \frac{1}{1+R_S/R_P}\left[J_S\left\{\exp\left(\frac{V-JR_SA}{nk_BT/e}\right)-1\right\} - \left(J_{ph}-\frac{V}{R_PA}\right)\right], \tag{1}$$

where k_B is the Boltzmann constant, T is the temperature in Kelvin, and e is the electronic charge. From Eq. (1), equations for J_{SC} and V_{OC} are easily derived:

$$V_{OC} = n\frac{k_BT}{e}\ln\left\{1+\frac{J_{ph}}{J_S}\left(1-\frac{V_{OC}}{J_{ph}R_PA}\right)\right\}, \tag{2}$$

$$J_{SC} = -\frac{1}{1+R_S/R_P}\left[J_{ph}-J_S\left\{\exp\left(\frac{|J_{SC}|R_SA}{nk_BT/e}\right)-1\right\}\right]. \tag{3}$$

Equations (1)–(3) usually need to be solved numerically, except for the case where R_S is very small and/or R_P is sufficiently large so that the effect from R_S or R_P may be ignored.

Another quantity of interest to evaluate the cell efficiency is the device fill factor FF which is defined by $J_{max}V_{max}/J_{SC}V_{OC}$, where V_{max} is the voltage at which the power output is maximized and $J_{max}=J(V_{max})$. It was shown by Shockley and Queisser[21] that the ideal fill factor FF_0 of a solar cell described by Eq. (1), in which $R_S=0$ and $R_P\to\infty$, can be expressed as a monotonically increasing function of the normalized open-circuit voltage ν_{OC} defined by $V_{OC}/(nk_BT/e)$. When $R_S>0$ and/or $R_P<\infty$, however, the actual FF for a given ν_{OC} is reduced from the ideal value $FF_0(\nu_{OC})$, as shown in Fig. 2. The following semiempirical expressions were shown to be good approximations of the numerically calculated values of FF for $\nu_{OC}>10$:[22,23]

$$FF_0 = \frac{\nu_{OC}-\ln(\nu_{OC}+0.72)}{\nu_{OC}+1}, \quad (r_S = 1/r_P = 0), \tag{4a}$$

$$FF_S = FF_0(1-1.1r_S)+0.19r_S^2, \quad (0\leqslant r_S\leqslant 0.4, 1/r_P=0), \tag{4b}$$

$$FF_{SP} = FF_S\left\{1-\frac{(\nu_{OC}+0.7)}{\nu_{OC}}\frac{FF_S}{r_P}\right\}, \quad (0\leqslant r_S+1/r_P\leqslant 0.4), \tag{4c}$$

in which r_S and r_P are normalized series and shunt resistances defined by R_S/R_{CH} and R_P/R_{CH}, respectively, in which R_{CH}, the characteristic resistance, is defined as $V_{OC}/(|J_{SC}|A)$. When both r_S and $1/r_P$ are larger than zero, the fill factor FF_{SP} can be calculated by substituting FF_S into Eq. (4c) after obtaining FF_S from Eq. (4b), assuming $1/r_P=0$. According to Ref. 23, this method gives reasonably close approximations of the numerically calculated results for $r_S+1/r_P\leqslant 0.4$ and $\nu_{OC}>10$, and its accuracy gets even better if one or both values of r_S and $1/r_P$ are small.[23] Note that the FF of the case where $r_S=0$ but $1/r_P\neq 0$ or FF_P, can also be described by Eq. (4c) with $FF_S=FF_0$, as long as $1/r_P\leqslant 0.4$.

The above expressions yield good approximations which are close enough in most cases for $\nu_{OC}>10$, but it may be beneficial to have more general expressions that are also applicable over a range of smaller values of ν_{OC}, especially for cells with relatively large n. Therefore, following the proce-

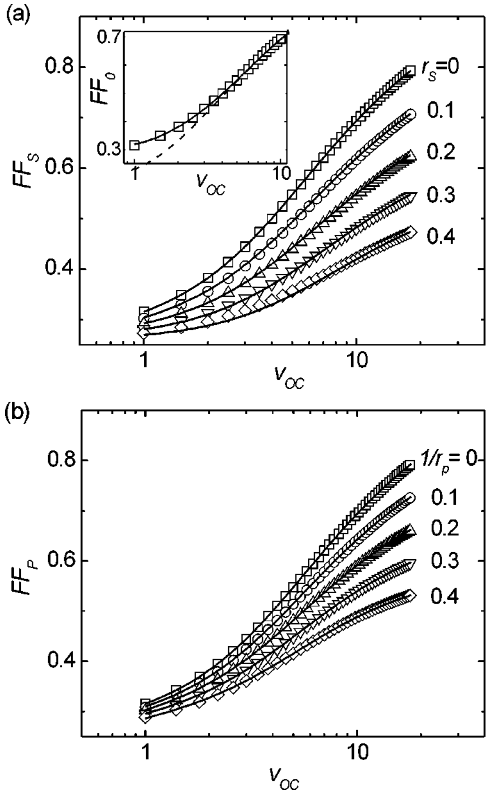

FIG. 2. Fill factor vs normalized open-circuit voltage ν_{OC} of a solar cell, following the equivalent circuit in Fig. 1 under the respective influence of (a) series resistance $R_S(\equiv FF_S)$ and (b) shunt resistance $R_P(\equiv FF_P)$. $\nu_{OC} = V_{OC}/(nk_BT/e), r_S = R_S/R_{CH}$, and $r_P = R_P/R_{CH}$ in which R_{CH}, characteristic resistance, is defined by $V_{OC}/(|J_{SC}|A)$. The open shapes represent the numerically calculated values obtained by the procedures described in Ref. 21. The solid lines represent the calculated values from the modified semiempirical equations summarized in Table I. FF_P is calculated from the equation for FF_{SP} with $r_S=0$. Inset: Zoomed view for fill factor in the absence of any resistance effect, FF_0. Dashed line: values obtained using Eq. (4a).

dure of Green[22] to numerically calculate FF, we propose the following modified equation for each case:

$$FF_j(\nu_{OC},\rho_j;a_j,b_j) = \left\{1 + a_j\rho_j \exp\left(-\frac{\nu_{OC}}{b_j}\right)\right\}FF_j^{(0)},$$
$$j = 0,\ S,\ \text{or SP}, \qquad (5)$$

in which $FF_j^{(0)}$ is the expression given in Eq. (4), with the subscript $j=0$, S, or SP corresponding to the same situation specified therein, (a_j,b_j) is a set of coefficients for each case, and $\rho_0=1$, $\rho_S=r_S$, and $\rho_{SP}=1/r_P$. It is emphasized that no assumption is imposed on J_{SC} or V_{OC} in the method presented in Ref. 22 for the numerical calculation of FF. In fact, it correctly accounts for a possible reduction in the magnitude of J_{SC} or V_{OC} due to resistances. With (a_j,b_j) summarized in Table I, these semiempirical expressions can be used as good approximations of the numerically calculated values for $\nu_{OC}\geqslant 1$. The validity of FF_{SP} obtained by Eq. (5) was checked for $\nu_{OC}\geqslant 1$ and for several sets of (r_S,r_P) fulfilling $r_S+1/r_P\leqslant 0.4$. It turned out that the relative error with respect to the numerically calculated values was mostly less than ±1% if one or both of r_S and $1/r_P$ are much less than 0.1, and that it was still within a few percents in the other cases. Therefore, Eq. (5) provides the approximation that is similar to Eq. (4), but with the extended range of ν_{OC} down to 1.

The knowledge of the equivalent circuit parameters for a given solar cell provides useful guidelines to further improve its performance. If specific physical effects in the device can be related to specific circuit parameters, and if these effects can be somehow controlled during device design and fabrication, then the equivalent circuit model teaches us how to optimize the circuit parameters to maximize the power conversion efficiency. In the following sections, the effects of these parameters on the electrical characteristics will be discussed in more details.

B. Effect of equivalent circuit parameters on electrical characteristics

From the analysis shown above, the influence of equivalent-circuit parameters on electrical characteristics can be quantitatively described. For example, it can be easily noted from Fig. 2 that a solar cell with a larger n will be subjected to a smaller fill factor than cells with the same V_{OC} but smaller n because the fill factor increases with the normalized open-circuit voltage. This situation can also be explained in terms of J_S. Note from Eq. (2) that ν_{OC} is a function only of J_{ph}/J_S when R_P is sufficiently high. If J_{ph} is the same for the cells under comparison, a cell with a larger J_S will have a smaller ν_{OC}, and therefore a smaller FF. Organic

TABLE I. Modified semiempirical equations for fill factors of solar cells described by the equivalent circuit shown in Fig. 1(b).

$$FF_j(\nu_{OC},\rho_j;a_j,b_j) = \left\{1 + a_j\rho_j \exp\left(-\frac{\nu_{OC}}{b_j}\right)\right\}FF_j^{(0)}(\nu_{OC},\rho_j), \quad \nu_{OC}\geqslant 1$$

j	Cases	ρ_j	a_j	b_j	$FF_j^{(0)}$
0	$r_S=1/r_P=0$	1	1.07	1.0	$\frac{\nu_{OC}-\ln(\nu_{OC}+0.72)}{\nu_{OC}+1}$
S	$0\leqslant r_S\leqslant 0.4, \quad 1/r_P=0$	r_S	1.30	2.0	$FF_0(1-1.1r_S)+0.19r_S^2$
SP	$0\leqslant r_S+1/r_P\leqslant 0.4$	$1/r_P$	0.75	1.5	$FF_S\left\{1-\frac{(\nu_{OC}+0.7)}{\nu_{OC}}\frac{FF_S}{r_P}\right\}$

solar cells can have open-circuit voltages that are comparable to or larger than those of inorganic *pn*-junction solar cells, but they often suffer from relatively large n and J_S. Their fill factors are therefore limited in many cases. For a photovoltaic (PV) cell showing $V_{OC}=500$ mV, for example, FF_0 at $T=300$ K would be 0.80 for $n=1$, but it drops to 0.69 for $n=2$.

As suggested in the equations given in Sec. III A, equivalent resistances can compromise the photovoltaic performance by reducing fill factors, $|J_{SC}|$, and V_{OC}. It is important to note that the effects of these resistances are relative, as it can be easily exemplified in their influences on *FF*. Observe that Eqs. (4) and (5) are functions of normalized resistances (r_S, r_P), rather than the absolute values of resistances (R_S, R_P). It is well illustrated in Eqs. (4b) and (4c) that the effect of R_S is more pronounced when $|J_{SC}|$ is large, while the effect of R_P exhibits the opposite trend. In other words, moderate values of the series resistance might have little effect on the fill factor in less-efficient solar cells in which $|J_{SC}|$ is moderate, but could become a more severe limiting factor in cells with higher photocurrents. $|J_{SC}|$ and V_{OC} are relatively insensitive to the values of the resistances in comparison to *FF* up to a certain point, but they can also be significantly reduced if R_SA becomes too large, or if R_PA becomes too small.[11]

The expressions given in Sec. III A are very useful not only in assessing the influence of the equivalent circuit parameters but also in analyzing the experimental data. When the equivalent circuit model is used in fitting experimental *J–V* curves, however, it is important to maintain only a minimal number of fitting parameters in order to obtain a more meaningful analysis. Note from Eqs. (2)–(5) that the five parameters J_S, n, J_{ph}, R_S, and R_P are linked with one another by the three constraints for V_{OC}, J_{SC}, and *FF*, all of which can be experimentally determined. Therefore, the independent parameters can be reduced to only two parameters. If R_S and R_P are given, for example, ν_{OC} and thereby $n[=eV_{OC}/(\nu_{OC}k_BT)]$ can be determined from the equation for *FF*. Then, J_S and J_{ph} can be determined from Eqs. (2) and (3). Therefore, one can fit the experimental *J–V* characteristics using only R_S and R_P as independent fitting parameters. In the following sections, we will use this method to extract the equivalent circuit parameters from our experimental data and discuss their influences on the device performance.

IV. RESULTS AND DISCUSSION

A. Photovoltaic response and its modeling using the simple equivalent circuit model

Figure 3 shows the electrical characteristics of a device ($A=0.13\pm0.01$ cm^2) with a geometry of ITO/pentacene (45 nm)/C_{60}(50 nm)/BCP(10 nm)/Al under illumination of the broadband light (350–900 nm), with I_L varied between 0 and 100 mW/cm^2. At $I_L=100\pm2$ mW/cm^2, $|J_{SC}|=15\pm1.4$ mA/cm^2, $V_{OC}=363\pm3$ mV, and $FF=0.50\pm0.01$, yielding a power conversion efficiency ($\eta=FF|J_{SC}|V_{OC}/I_L$) of 2.7 ± 0.4%. Figure 4 summarizes the dependence of the photovoltaic parameters versus intensity I_L. $|J_{SC}|$ shows good

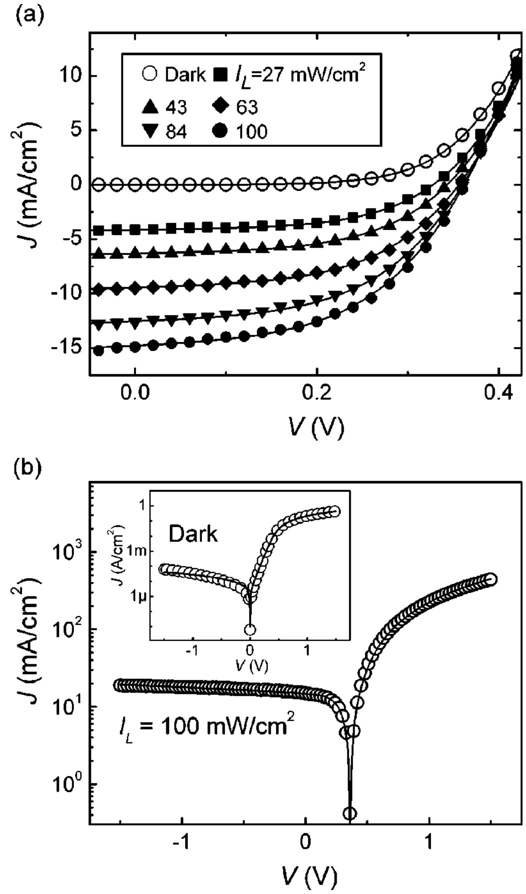

FIG. 3. (a) *J–V* characteristics of ITO/pentacene (45 nm)/C_{60}(50 nm)/BCP(10 nm)/Al under illumination of the broadband light (350–900 nm) at varying light intensities I_L (closed shapes) and in the dark (open circles). (b) Semilogarithmic *J–V* curves at $I_L=100$ mW/cm^2 (Inset: in the dark. The solid lines in (a) and (b) are the fitting curves for each case, obtained by the simple equivalent circuit model. Fitting parameters are summarized in Table II.

linearity with respect to I_L with the power fit of $0.151\,(\mathrm{A/W})I_L^{0.998}$ [dashed line in Fig. 4]. V_{OC} increases slightly with I_L while *FF* decreases, which makes η stay relatively constant.

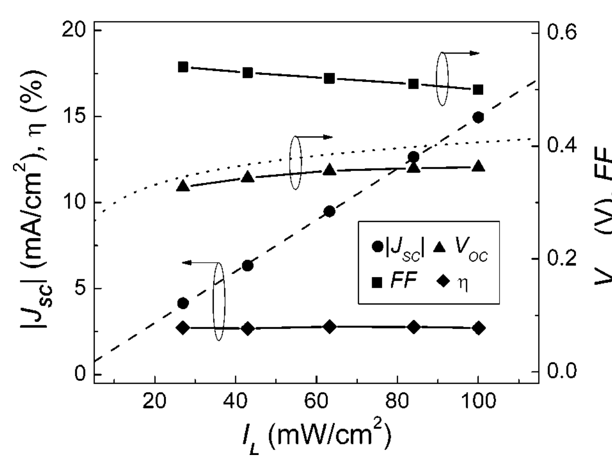

FIG. 4. Trends of photovoltaic parameters vs I_L. The solid lines are guides to the eye. Dashed line: power fit for $|J_{SC}|$, that is, $|J_{SC}|=0.151(\mathrm{A/W})I_L^{0.998}$. Dotted line: V_{OC} calculated from the relation for an ideal *pn*-junction cell.

TABLE II. Photovoltaic parameters vs light intensity (I_L) and fitting results using the equivalent circuit shown in Fig. 1(b) (T=300 K).

I_L (mW/cm^2)	$\lvert J_{SC}\rvert$ (mA/cm^2)	V_{OC} (V)	FF	η (%)	J_S (μA/cm^2)	n	R_SA (Ω cm^2)	R_PA (Ω cm^2)
Dark					2.3	1.8	2.15	40,100
27	4.2	0.328	0.54	2.72	12	2.2	2.19	1,176
43	6.4	0.344	0.53	2.68	20	2.3	2.09	780
63	9.5	0.356	0.52	2.78	29	2.4	2.08	515
84	12.6	0.361	0.51	2.77	42	2.5	2.04	408
100	15.0	0.363	0.50	2.71	54	2.5	2.04	328

To parameterize the current–voltage characteristics of these cells at a given intensity, we used the equivalent circuit model shown in Fig. 1(b). Fitting to the model was done based on discussion given in Sec. III B. First, estimation for $R_S(\equiv R_S^{\text{est}})$ and $R_P(\equiv R_P^{\text{est}})$ were made from the inverse slopes of the forward and reverse characteristics, respectively.[14] $J_{\text{ph}}=\lvert J_{SC}\rvert$ was assumed for simplicity. According to Eq. (3), this is a good approximation as long as $\lvert J_{SC}\rvert R_SA$ is not significantly larger than $n(k_BT/e)$, within the range of the illumination level of interest. Using these values, estimation for J_S and n could be directly made by solving Eqs. (2) and (5), even without a further fitting process. The parameters obtained in this way can serve as guidelines that are accurate enough, in many practical cases within error bound. However, the method using R_SA from the inverse slope of the forward characteristic can slightly overestimate R_SA because

$$\left(\frac{dJ}{dV}\right)^{-1} \approx R_SA + n\frac{kT}{eJ} > R_SA, \quad (V \gg V_{OC}), \tag{6}$$

and therefore result in errors in the forward bias region. Therefore, we varied R_S as a fitting parameter, with R_P fixed at $R_P{}^{\text{est}}$, and obtained (J_S,n) fulfilling Eqs. (2) and (5) for each set of (R_S,R_P) to find the set of parameters minimizing the sum of the squared errors (SSE) defined by

$$\text{SSE} = \sum_V \left[\{\log(\lvert J(V)\rvert) - \log(\lvert J_{\text{Fit}}(V)\rvert)\}^2 + \{J(V) - J_{\text{Fit}}(V)\}^2\right] \tag{7}$$

over the range of $-1.5\text{ V} < V < 1.5\text{ V}$. $J_{\text{Fit}}(V)$ is the current density generated by the model. The SSE defined in this way was taken from Ref. 15, and was found to be useful because the logarithmic terms can help avoid overweighing the forward bias region, which can sometimes lead to unsatisfactory fitting results which overlook the photovoltaic and reverse bias regions. Our method was not very sensitive to the choice of SSE for data obtained under illumination because the parameters are determined in such a way that the FF and V_{OC} are matched to the experimental results, but this SSE was used in particular for fitting the data measured in the dark. R_P may also be set as a fitting parameter, but a fixed value of $R_P=R_P{}^{\text{est}}$ resulted in a sufficiently adequate fit over the voltage range used. The fitting curves for dark and for each illumination level are represented by the solid lines in Fig. 3(a), and the parameters extracted from the best fitting results are summarized in Table II. Semilogarithmic curves shown for dark and $I_L=100$ mW/cm^2 in Fig. 3(b) demonstrate that these fits are in good agreement with experimental data throughout the voltage range used. These tight fits obtained at various light intensities suggest that this simple equivalent circuit model is appropriate for a given light intensity. It is advised that acceptable fit may also be obtained for a range of $\{J_S,n,R_S\}$, depending on the accuracy of experimental data. For example, at $I_L=100$ mW/cm^2,$\{J_S=54\mp 16$ μA/cm^2, $n=2.5\mp 0.15$, $R_SA=2.04\pm 0.04$ Ω cm$^2\}$ can produce a J–V curve that satisfies $FF=0.50\pm 0.01$, without change in V_{OC} when J_{ph} and R_P are set as the same values shown in Table II.

With the knowledge of the diode parameters, their influence on the electrical characteristics can be studied. For instance, at $I_L=63$ mW/cm^2, our device yields an experimental fill factor of $FF=0.52$ and an experimental open-circuit voltage of $V_{OC}=356$ mV. With an ideality factor of $n=2.4$ extracted from the fitting procedures, a value of $\nu_{OC}=5.73$ at $T=300$ K can be calculated, yielding a value of $FF_0=0.576$ using Eq. (5). The same V_{OC} with $n=1(n=1.5)$ would result in FF_0 of 0.75 (0.68). Since $R_{CH}A$ of this device is calculated to be 37.5 Ω cm^2 from the experimental values of J_{SC} and V_{OC}, r_S and r_P have values of 0.0555 and 13.7, respectively. From Eq. (5), one can evaluate that the effect of R_S results in $FF_S=0.544$, which corresponds to a reduction by 5.6% from the ideal fill factor FF_0. If we also include the effect of R_P using the equation for FF_{SP} in Eq. (5) as explained in Sec. III A, the resultant FF is then calculated to be 0.52, which corresponds to a reduction by 4.4% from the FF_S.

B. Extended equivalent circuit for simulation of the light intensity dependence

While the simple equivalent circuit shown in Fig. 1(b) provides quantitative information on the effect of each resistance on the device fill factor at each illumination level, it was not possible to fit our experimental data over a range of different I_L without a significant change in the diode parameters (J_S,n) and in shunt resistance R_P, which is in contrast to an ideal pn-junction solar cell. Similar phenomena were also reported in polymer blend bulk heterojunction solar cells,[15,18] and in small molecular weight multilayer cells.[3,17] Note in Figs. 5(a) and 5(b) that n varies when the cell is under illumination or in the dark, and that J_S and $1/R_P$ increase with intensity I_L while R_S remains relatively unchanged. It is seen that $(1/R_P-1/R_{P0})A^{-1}$ can be well fitted by γI_L in which R_{P0} is the shunt resistance measured in the dark and $\gamma=0.030$ Ω^{-1}W^{-1}. In addition, the dependence of

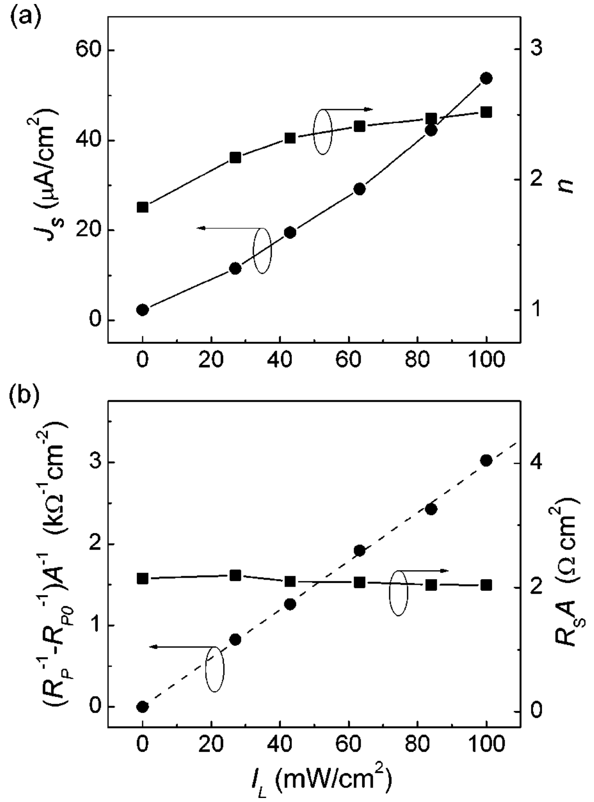

FIG. 5. (a) $(1/R_PA-1/R_{P0}A)$ and (b) (J_S-J_{S0}) and n vs I_L. R_{P0} and J_{S0} are the shunt resistance and the reverse saturation current density in the dark, respectively. The dashed line is the result of the linear fit for the inverse of shunt resistance, that is, $(1/R_PA-1/R_{P0}A)=0.030(\Omega^{-1}\mathrm{W}^{-1})I_L$. The solid lines are guides to the eye.

V_{OC} on I_L was different from the typical logarithmic relation (dotted line in Fig. 4) observed in typical inorganic *pn*-junction cells,[11] that is, Eq. (2) in which n and J_S are substituted with n_0 and J_{S0}, which are the ideality factor and the reverse saturation current density obtained in the dark, respectively.

In order to take into account this unconventional light dependence, we propose to modify the equivalent circuit and to incorporate an additional shunt resistance (R_{PL}) and a second diode, as shown in Fig. 6. In this modified circuit, the value of R_{PL}, and the reverse saturation current density J_{SL} and ideality factor n_L of the second diode, may be regarded as functions of light intensity in general. The current–voltage characteristic for such circuit is then given by

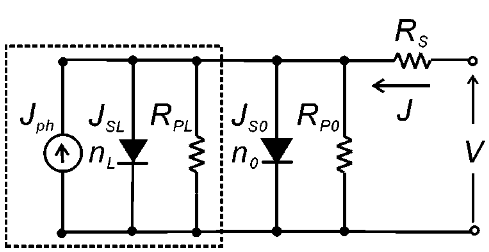

FIG. 6. Modified equivalent circuit containing the additional shunt resistance (R_L) and diode (J_{SL},n_L) the parameters of which may be dependent on light intensity. Parameters with the subscript "0" indicate those obtained in the dark. Components with the intensity-dependent parameters are enclosed by the dashed line.

$$J = J_{\mathrm{S0}}\left(\exp\left(\frac{V'}{n_0k_BT/e}\right)-1\right)+\frac{V'}{R_{\mathrm{P0}}A} + J_{\mathrm{SL}}\left(\exp\left(\frac{V'}{n_Lk_BT/e}\right)-1\right)-J_{\mathrm{ph}}+\frac{V'}{R_{\mathrm{PL}}A}, \tag{8}$$

where $V'\equiv V-JR_SA$, and R_{P0} is the shunt resistance determined in the dark. The double-diode model was introduced previously to account for the recombination current in the dark characteristics of inorganic solar cells,[13] but no light dependence was usually assumed. The added shunt resistance can describe various bulk photoconductive effects.[3,14,15]

In a similar way described in Sec. IV A, the experimental *J–V* curves were fitted to Eq. (8) at each illumination level, with R_S set as a fitting parameter and with the net shunt resistance $R_P=(1/R_{\mathrm{P0}}+1/R_{\mathrm{PL}})^{-1}$ fixed at the same value tabulated in Table II. A set of J_{SL} and n_L matching the experimental V_{OC} and *FF* was numerically calculated for each set of (R_S,R_P) during the fitting process.[24] The n_0 of 1.8 and J_{S0} of 2.3 $\mu\mathrm{A/cm}^2$ were used as specified for the dark condition in Table II. As demonstrated in Fig. 7(a), fitting with the modified equivalent circuit also resulted in very tight fits to the experimental data. The best fitting results were obtained with $n_L=3.1\pm0.3$ and $R_SA=2.2\pm0.1\ \Omega\,\mathrm{cm}^2$ in the range of illumination intensities studied. (See Table III.) Figure 7(b) shows that J_{SL} increases with I_L, similar to the trend of J_S shown in the single-diode equivalent circuit model. When the dependence of J_{SL} on I_L is assumed linear, the linear fits for $J_{\mathrm{ph}},J_{\mathrm{SL}}$, and $1/R_{\mathrm{PL}}$ result in the final electrical characteristic which is expressed as a function of I_L as follows:

$$J = J_{\mathrm{S0}}\left(\exp\left(\frac{V'}{n_0k_BT/e}\right)-1\right)+\frac{V'}{R_{\mathrm{P0}}A} + I_L\left[\alpha\left(\exp\left(\frac{V'}{n_Lk_BT/e}\right)-1\right)-\beta+\gamma V'\right], \tag{9}$$

in which $V'=V-JR_SA, R_{\mathrm{P0}}A=40\,100\ \Omega\,\mathrm{cm}^2, \alpha=7.5\times10^{-4}\ \mathrm{A/W}, \beta=0.15\ \mathrm{A/W}$, and $\gamma=0.030\ \Omega^{-1}\mathrm{W}^{-1}$, where $J_{\mathrm{SL}}(I_L)\equiv\alpha I_L, J_{\mathrm{ph}}(I_L)\equiv\beta I_L$, and $[R_{\mathrm{PL}}(I_L)A]^{-1}\equiv\gamma I_L$.[25] R_SA and n_L were fixed at 2.2 $\Omega\,\mathrm{cm}^2$ and 3.1, respectively, as their variations were relatively small.

As shown in Fig. 8, the experimental photovoltaic parameters as a function of I_L are in very good agreement with the model prediction given by Eq. (9). In addition, one can use this model to gain insight into the relative effects of the different equivalent circuit parameters. In other words, one can simulate hypothetical cell photovoltaic parameters in different ideal situations. Figure 8 describes how the *FF*, V_{OC}, and η are influenced when R_S,R_{PL}, and J_{SL} are sequentially added to the ideal cell in which all of these components are absent. It can be easily noted that R_S and J_{SL} are the major factors limiting the cell efficiencies at high intensities. These effects may also be well illustrated by observing changes in simulated *J–V* characteristics upon addition of these parameters. For example, the dashed line in Fig. 7(a) shows a simulated *J–V* characteristic at $I_L=100\ \mathrm{mW/cm}^2$ of a cell in which the effects of the dependence of the circuit parameters

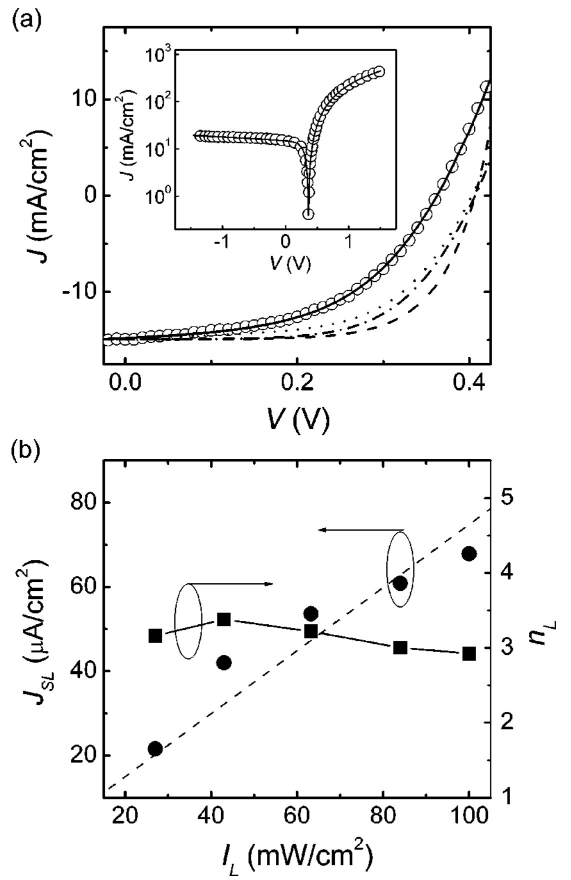

FIG. 7. (a) Best-fitting result using the modified equivalent circuit model. Open circles: experimental data at $I_L = 100\ \mathrm{mW/cm^2}$. Solid line: fitting curve. Inset: wide-range plot in semilogarithmic scale. Hypothetical *J–V* curves are presented to illustrate the effect of the series resistance R_S, the additional shunt resistance R_{PL}, and the additional diode (J_{SL}, n_L) on the electrical characteristics; dashed line: case where there is no additional diode, and $R_S=0$ and $R_P=R_{P0}$. Dash-dotted line: no additional diode, and $R_P = R_{P0}$ but $R_S A \neq 0$. Dotted line: no additional diode but $R_P = (R_{P0}^{-1} + R_{PL}^{-1})^{-1}$ and $R_S A \neq 0$. In all cases, $R_{P0}A = 40\,100\ \Omega\ \mathrm{cm^2}$, and $R_S A = 2.14\ \Omega\ \mathrm{cm^2}$ unless specified as zero. For details on fitting results, refer to Table III. (b) J_{SL} and n_L vs I_L obtained by the fitting process using the modified equivalent circuit. The dashed line is the result of a linear fit for J_{SL}, that is, $J_{SL} = [7.5\times10^{-4}(\mathrm{A/W})]I_L$. The solid lines are guides to the eye.

(R_P, J_S) on the light intensity have been eliminated, and in which $R_S=0$. Under such conditions, one would observe an open-circuit voltage V_{OC} of 407 mV, a fill factor *FF* of 0.67, and a power conversion efficiency η of 4.1% at I_L

TABLE III. Fitting results using the modified equivalent circuit shown in Fig. 6.

$J_{S0} = 2.3\ \mu\mathrm{A/cm^2}$, $n_0 = 1.8$, $R_{P0}A = 40\,100\ \Omega\ \mathrm{cm^2}$

I_L $(\mathrm{mW/cm^2})$	J_{SL} $(\mu\mathrm{A/cm^2})$	n_L	$R_S A$ $(\Omega\ \mathrm{cm^2})$	$R_{PL}A$[a] $(\Omega\ \mathrm{cm^2})$
27	22	3.2	2.30	1210
43	42	3.4	2.22	795
63	54	3.2	2.20	522
84	61	3.0	2.14	412
100	68	2.9	2.14	331

[a] R_{PL} was calculated from $R_{PL} = (1/R_P - 1/R_{P0})^{-1}$ in which R_P is the net shunt resistance tabulated in Table II.

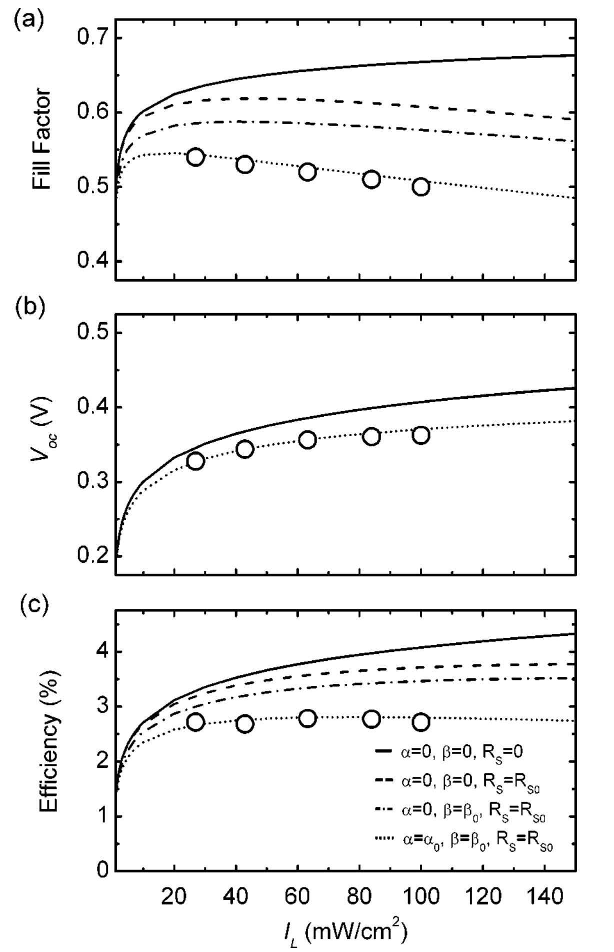

FIG. 8. Simulated photovoltaic parameters as a function of light intensity I_L: (a) *FF*, (b) V_{OC}, and (c) efficiency. In all cases, the open circles are experimental data, and the lines are the calculated values using Eq. (9), with α, γ, and R_S as specified in the bottom part of the figure. Unless specified as zero, $\alpha \equiv J_{SL}(I_L)/I_L = 7.5\times10^{-4}\ \mathrm{A/W}$, $\gamma \equiv [R_{PL}(I_L)A]^{-1}/I_L = 0.030\ \Omega^{-1}\mathrm{W}^{-1}$, $\beta \equiv J_{ph}(I_L)/I_L = 0.15\ \mathrm{A/W}$, and $R_S A = 2.2\ \Omega\ \mathrm{cm^2}$ were used. J_{S0}, n_0, and $R_{P0}A$ are $2.3\ \mu\mathrm{A/cm^2}$, 1.8, and $40\,100\ \Omega\ \mathrm{cm^2}$, respectively.

$=100\ \mathrm{mW/cm^2}$. If one maintains only the effects of the series resistance, the efficiency η reduces to 3.7%, due to a decrease in *FF*. If the effects from both R_{PL} and R_S are included but the dependence of the reverse saturation current on light intensity is ignored, η reduces to 3.4%. These values of efficiency have to be compared with the efficiency of η of 2.7% that is measured at $I_L = 100\ \mathrm{mW/cm^2}$ in our devices. This analysis shows that the effective increase of the reverse saturation current density with illumination intensity results in a decrease of both V_{OC} and *FF*, which accounts for half of the total reduction in efficiency from a maximum ideal value of 4.1% to the measured value of 2.7%. Possible explanations for the origin of the dependence of the circuit parameters on light intensity may include the field-dependent recombination of photogenerated carriers, as was suggested by Schilinsky *et al.*[15] in bulk heterojunction cells.

In Fig. 8, one can also note that the effect of R_{PL} on *FF* and efficiency is more significant than that of R_S in low light intensities but it stays almost constant upon an increase in I_L even though the net R_P continues to decrease. It is due to the fact that the normalized shunt resistance r_P remains relatively unchanged because the decrease in R_P with I_L is compensated with an increase in $|J_{SC}|$. On the other hand, the effects of R_S and J_{SL} become more significant as I_L increases, indicating they are among the most important parameters that need to be controlled in order to ultimately achieve a highly efficient solar energy conversion in this type of cells.

V. CONCLUSIONS

In summary, the electrical characteristics of efficient solar cells based on pentacene/C_{60} heterojunctions were studied in the dark and under illumination for different light intensities. Using the simple equivalent circuit model, the current–voltage characteristics of these cells in the dark and under illumination could be parameterized. The set of parameters was $\{J_S, n, R_P, R_S, J_{ph}\}$, where J_{ph} is the photocurrent, J_S is the reverse saturation current of the diode, n is the ideality factor of the diode, R_P is the shunt resistance, and R_S is the series resistance. In contrast to an ideal inorganic *pn*-junction solar cell for which these parameters are constant except for the photocurrent which is a linear function of the light intensity, we observed significant changes in the diode parameters (J_S, n) and shunt resistance R_P upon variation in the intensity of the illumination. To provide for a model that can simulate the current–voltage characteristics of our cells under any illumination within the range that was studied, we used a modified equivalent circuit. In this circuit, the diode and the shunt resistance are each replaced by two components: one diode describing the properties measured in the dark with fixed parameters (J_{S0}, n_0); and a second diode with parameters (J_{SL}, n_L) taking into account the intensity dependence of the diode parameters. Likewise, a second shunt resistance R_{PL} is added in parallel to the shunt resistance R_{P0} measured in the dark. Note that in this modified model, the new set of parameters is $\{J_{S0}, n_0, R_{P0}, R_S, J_{SL}, n_L, R_{PL}, J_{ph}\}$. The subset of parameters $\{R_{PL}, J_{ph}\}$ are all functions of the intensity, which have been determined by applying the simple equivalent circuit to the cells under five different illumination intensities (Figs. 4 and 5). The subset of parameters $\{J_{S0}, n_0, R_{P0}\}$ is taken from the fitting results obtained in the dark by the simple equivalent circuit model. That leaves us with three undetermined parameters. However, the number of fitting parameters can be reduced to one, namely, R_S. For a given value of R_S the other two parameters $\{J_{SL}, n_L\}$ could be evaluated in order to match the experimental values of *FF* and V_{OC}. For the pentacene /C_{60} cells investigated in this study, a good fit to the current–voltage characteristics was found over the range of light intensities up to 100 mW/cm^2, using the modified model with $R_SA = 2.2 \pm 0.1\ \Omega\ \mathrm{cm}^2$, $J_{SL} = \alpha I_L$ with $\alpha = 7.5 \times 10^{-4}$ A/W, and $n_L = 3.1 \pm 0.3$. Within this model, we were able to show that the light intensity dependence of these parameters is partly responsible for a reduction of the overall performance of the solar cells. We were also able to discuss their relative influence on power conversion efficiency as a function of the illumination intensity. Our study suggests that the efficiency of these cells can be significantly further improved if these various effects can be directly connected to physical processes taking place in these excitonic cells such as those already mentioned in the literature,[3,14,15] and if these physical processes can be controlled during cell design and fabrication. As it was demonstrated in pentacene field-effect transistors that the transport properties can be improved via interfacial engineering,[26,27] for example, if one can identify the interactions between the organic film and the adjacent layer that will lead to a change in film morphology, favoring an increase of mobility and/or reduction of contact resistance, this can potentially lead to a decrease in the series resistance upon careful control of the related processes. Such studies are currently under way.

ACKNOWLEDGMENTS

This material is based upon the work supported in part by the STC Program of the National Science Foundation under Contract No. DMR-0120967, by the Office of Naval Research, by the National Renewable Energy Laboratory, and by an NSF CAREER program (B.K.).

[1]C. W. Tang, Appl. Phys. Lett. **48**, 183 (1986).
[2]P. Peumans and S. R. Forrest, Appl. Phys. Lett. **79**, 126 (2001).
[3]J. Xu, S. Uchida, B. P. Rand, and S. R. Forrest, Appl. Phys. Lett. **84**, 3013 (2004).
[4]S. E. Shaheen, C. J. Brabec, N. S. Sariciftci, F. Padinger, T. Fromherz, and J. C. Hummelen, Appl. Phys. Lett. **78**, 841 (2001).
[5]P. Schilinsky, C. Waldauf, and C. J. Brabec, Appl. Phys. Lett. **81**, 3013 (2002).
[6]F. Padinger, R. S. Rittberger, and N. S. Sariciftci, Adv. Funct. Mater. **13**, 85 (2003).
[7]W. U. Huynh, J. J. Dittmer, and A. P. Alivisatos, Science **295**, 2425 (2002).
[8]J. Krüger, R. Plass, L. Cevey, M. Piccirelli, U. Bach, and M. Gratzel, Appl. Phys. Lett. **79**, 2085 (2001).
[9]K. M. Coakley and M. D. McGehee, Appl. Phys. Lett. **83**, 3380 (2003).
[10]S. Yoo, B. Domercq, and B. Kippelen, Appl. Phys. Lett. **85**, 5427 (2004).
[11]M. A. Green, *Solar Cells* (Prentice-Hall, Engtewood Cliffs, NJ, 1982).
[12]A. R. McGhie, A. F. Garito, and A. J. Heeger, J. Cryst. Growth **22**, 295 (1974).
[13]S. M. Sze, *Physics of Semiconductor Devices* (Wiley, New York, 1981).
[14]W. U. Huynh, J. J. Dittmer, N. Teclemariam, D. J. Milliron, and A. P. Alivisatos, Phys. Rev. B **67**, 115326 (2003).
[15]P. Schilinsky, C. Waldauf, J. Hauch, and C. J. Brabec, J. Appl. Phys. **95**, 2816 (2004).
[16]T. Aeronouts, W. Greens, J. Poortmans, S. Borghs, and R. Mertens, Thin Solid Films **403-404**, 297 (2002).
[17]J. Rostalski and D. Meissner, Sol. Energy Mater. Sol. Cells **63**, 37 (2000).
[18]I. Riedel, J. Parisi, V. Dyakonov, L. Lusten, D. Vanderzande, and J. C. Hummelen, Adv. Funct. Mater. **14**, 38 (2004).
[19]C. J. Brabec, S. E. Shaheen, C. Winder, N. S. Sariciftci, and P. Denk, Appl. Phys. Lett. **80**, 1288 (2002).
[20]Although the series resistance in the equivalent circuit model shown in Fig. 1(b) is the resultant sum of all the resistances from the different sources, these effects can be separated from each other in a carefully designed experiment. For example, if the thickness of a semiconductor layer is varied while all the other conditions remain unchanged, the portion from the bulk resistivity of the material can be separated from the contact resistance, as demonstrated in Ref. 16. Resistances due to interconnections and probe lines may be assumed negligible if one uses a so-called four-wire connection scheme which is available in most of the source-measure units such as Keithley 2400 used in this study.
[21]W. Shockley and H. J. Queisser, J. Appl. Phys. **32**, 510 (1961).
[22]M. A. Green, Solid-State Electron. **24**, 788 (1981).
[23]M. A. Green, Sol. Energy Mater. Sol. Cells **7**, 337 (1982).
[24]Since Eq. (5) is good for an equivalent circuit model with a single diode, *FF* was calculated by finding the condition maximizing the product of V and $J(V)$ in $0 < V < V_{OC}$.
[25]This observation is in line with the study on the characteristics of a multilayer CuPc/C_{60} solar cell reported in Ref. 3. In that report, the similar pattern of results were obtained by fitting the "net photocurrent" defined by the difference in $J(V)$ under illumination and in the dark. While

this method is adequate as their cells have very small $R_S A$, it can lead to an underestimation of photocurrent at $0 < V < V_{OC}$ when the effect of the $R_S A$ can no longer be ignored, as its influence on electrical characteristics is different between dark and illuminated conditions and moreover becomes more significant when the light intensity increases.

[26]M. Shtein, J. Mapel, J. B. Benziger, and S. R. Forrest, Appl. Phys. Lett. **81**, 268 (2002).
[27]T. W. Kelley, L. D. Boardman, T. D. Dunbar, D. V. Muyres, M. J. Pellerite, and T. P. Smith, J. Phys. Chem. B **107**, 5877 (2003).